Divergent regulation of insulin-like growth factor binding protein genes in cultured Atlantic salmon myotubes under different models of catabolism and anabolism

Accepted Manuscript

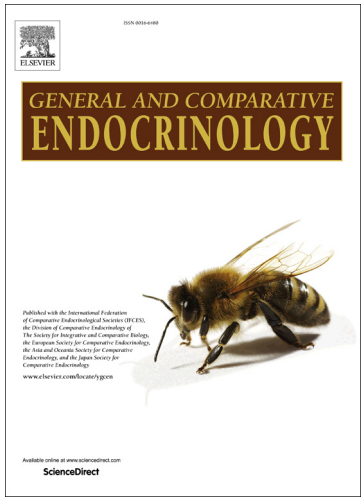

Divergent regulation of insulin-like growth factor binding protein genes in cultured Atlantic salmon myotubes under different models of catabolism and anabolism

Daniel Garcia de la Serrana, Eduardo N. Fuentes, Samuel A.M. Martin, Ian A. Johnston, Daniel J. Macqueen

PII: S0016-6480(16)30399-9
DOI: http://dx.doi.org/10.1016/j.ygcen.2017.01.017
Reference: YGCEN 12565

To appear in: *General and Comparative Endocrinology*

Received Date: 18 November 2016
Revised Date: 12 January 2017
Accepted Date: 17 January 2017

Please cite this article as: Garcia de la Serrana, D., Fuentes, E.N., Martin, S.A.M., Johnston, I.A., Macqueen, D.J., Divergent regulation of insulin-like growth factor binding protein genes in cultured Atlantic salmon myotubes under different models of catabolism and anabolism, *General and Comparative Endocrinology* (2017), doi: http://dx.doi.org/10.1016/j.ygcen.2017.01.017

Divergent regulation of insulin-like growth factor binding protein genes in cultured Atlantic salmon myotubes under different models of catabolism and anabolism

Daniel Garcia de la Serrana *^ [a], Eduardo N. Fuentes ^[a,b,c], Samuel A.M. Martin [c], Ian A. Johnston [a], Daniel J. Macqueen * [c]

[a] School of Biology, Scottish Oceans Institute, University of St Andrews, Fife KY16 8LB, Scotland, United Kingdom.

[b] Interdisciplinary Center for Aquaculture Research (INCAR), Víctor Lamas 1290, PO Box 160-C, Concepción, Chile.

[c] Institute of Biological and Environmental Sciences, University of Aberdeen, Tillydrone Avenue, Aberdeen, AB24 2TZ, Scotland, United Kingdom.

[*] Corresponding authors:

Daniel Garcia de la Serrana. Email address: dgdlsc@st-andrews.ac.uk

Daniel J. Macqueen. Email address: daniel.macqueen@abdn.ac.uk

^Authors contributed equally

Running title: Igfbp expression and remodelling of fish myotubes

Abstract

Much attention has been given to insulin-like growth factor (Igf) pathways that regulate the balance of skeletal muscle protein synthesis and breakdown in response to a range of extrinsic and intrinsic signals. However, we have a less complete understanding of how the same signals modulate muscle mass upstream of such signalling, through a family of functionally-diverse Igf-binding proteins (Igfbps) that modify the availability of Igfs to the cell receptor Igf1r. We exposed cultured myotubes from Atlantic salmon (*Salmo salar* L.) to treatments recapturing three catabolic signals: inflammation (interleukin-1β), stress (dexamethasone) and fasting (amino acid deprivation), plus one anabolic signal: recovery of muscle mass post-fasting (supplementation of fasted myotubes with Igf-I and amino acids). The intended phenotype of treatments was confirmed by significant changes in myotube diameter and immunofluorescent staining of structural proteins. We quantified the mRNA-level regulation of the full expressed Igf and Igfbp gene complement across a post-treatment time course, along with marker genes for muscle structural protein synthesis, as well as muscle breakdown, via the ubiquitin-proteasome and autophagy systems. Our results highlight complex, non-overlapping responses of Igfbp family members to the different treatments, suggesting that the profile of expressed Igfbps is differentially regulated by distinct signals promoting similar muscle remodelling phenotypes. We also demonstrate divergent regulation of salmonid-specific gene duplicates of *igfbp5b1* and *igfbp5b2* under distinct catabolic and anabolic conditions. Overall, this study increases our understanding of the regulation of Igfbp genes in response to signals that promote remodelling of skeletal muscle.

Keywords: Skeletal muscle, Myotubes, Cell culture, Insulin-like growth factor system; Igf binding proteins, Atlantic salmon, Dexamethasone, Interleukin-1β, amino acids.

1. Introduction

Skeletal muscle growth involves a net accumulation of protein, with rates of protein synthesis exceeding that of degradation. One of the key systems regulating this balance is the insulin-like growth factor (Igf) - phosphoinositide 3 kinase (Pi3k) - Akt/protein kinase B (Akt) - mammalian target of rapamycin (mTor) pathway. The hormones Igf-I and Igf-II act as endocrine factors (Laron, 1996; Wood et al. 2005), but are also released locally by tissues, including skeletal muscle (Schiaffino and Mammucari, 2011). Both Igfs are major anabolic factors in skeletal muscle, promoting protein synthesis, whilst inhibiting atrophy (Firth and Baxter 2002; Wood et al., 2005; Duan et al., 2010). The binding of Igf hormones to Igf1r, their primary cell-membrane receptor, initiates an intracellular phosphorylation cascade that activates Pi3k complexes and key downstream signalling molecules, most notably Akt (Hers et al., 2011), which in turn activates mTor/Raptor complexes – inducing an increase in protein translation via regulation of P70s6 kinases and Eif4ebp1 family members (Wang and Proud, 2006). Regulation of Igfs in the extracellular environment (e.g. circulation and extracellular matrix) provides an important level of upstream control to these signalling events and is primarily governed by a family of functionally-diverse Igf binding proteins (Igfbp-1 to 6) present in all vertebrates, but particularly well-characterized in mammals. These Igfbps can either restrict Igf hormones from Igf1r or facilitate the accumulation of Igf on cell membranes in proximity to Igf1r (Firth and Baxter, 2002; Duan and Xu, 2005). Accordingly, the expression of different Igfbp subtypes allows for both inhibition and potentiation of Igf-signalling, which may allow appropriate muscle mass regulation according to signals favouring catabolism or anabolism.

The ubiquitin-proteasome and autophagy-lysosome systems are major pathways leading to skeletal muscle protein degradation (Schiaffino et al., 2013). The ubiquitin-proteasome pathway is crucial for removal of sarcomeric proteins following muscle damage, in response to changes in muscle activity, or upon remodelling of muscle mass (Murton et al., 2008). Proteins to be degraded by the proteasome

are cross-linked by muscle-specific E3-ubiquitin ligases to ubiquitin (Schiaffino et al., 2013). The main recognized E3-ubiquitin ligases in skeletal muscle, employed widely as markers of muscle catabolism, are F-box only protein 32 (Fbxo32) (also called Atrogin-1 or Mafbx) and members of the muscle RING-finger (Murf) family (Glass 2005, Sacheck et al., 2007; Johnston et al. 2011; Macqueen et al. 2014). The autophagy-lysosome pathway also plays a key role in the turnover of cellular organelles during both normal and stressful conditions (Schiaffino et al., 2013). The Igf pathway negatively regulates both degradation pathways through activated Akt, which phosphorylates Foxo transcription factors, blocking their nuclear entry (Tzivion et al., 2011), causing downregulation of target genes including *mafbx* and *murf1* (Glass, 2005), as well as key genes involved in lysosome formation and autophagy (Mammucari et al., 2007). The impact of external and endogenous signals driving skeletal muscle breakdown on these intracellular pathways is well characterized (Bonaldo and Sandri, 2013). For example, glucocorticoids such as the cortisol-analogue dexamethasone, increase the transcription of *murf1*, *mafbx* and autophagy genes, while inhibiting protein synthesis by blocking mTor function (Braun and Marks, 2015). In addition, cytokines, such as Tnfα and IL-1β increase the transcription of E3-ubiquitin ligases, including *murf1* via Nfκβ pathways (Glass, 2005; Pooley et al., 2013). Finally, fasting stimulates protein degradation by repressing Akt activation, leading to FoxO-mediated transcriptional upregulation of both E3-ubiquitin ligases and macro-autophagy genes (e.g. Sandri et al., 2004; Southgate et al., 2007; Calnan and Brunet, 2008; Seiliez et al. 2010; Shimizu et al., 2011).

Comparatively less is known about the role of Igfbps in skeletal muscle under such catabolic signals, particularly in teleost fish, where remodelling of muscle mass occurs routinely during the life cycle for reallocation of energy and amino acids between tissues (Johnston et al., 2011). For example, many teleosts undergo seasonal cycles of muscle wasting associated with migration and/or the mobilisation of amino acids to build gonadal tissue, followed by recovering after spawning (e.g. James and Johnston, 1998; Mommsen, 2004). Interestingly, in teleosts the Igfbp family is

105 characterized by additional gene duplicates (paralogues) of Igfbp1-6 retained from a whole genome
106 duplication (WGD) event ancestral to all teleosts (i.e. Igfbp1a/b, 2a/b, 3a/b, 5a/b and 6a/b) (Ocampo
107 Daza et al. 2011; Johnston et al. 2011; Macqueen et al. 2013). Additionally, in the salmonid family of
108 teleosts (the focus of the current study), the Igfbp family consists of no less than nineteen unique
109 genes (Macqueen et al. 2013; Lappin et al. 2016), owing to the retention of additional paralogues
110 from a salmonid-specific WGD ~95 Ma (Macqueen and Johnston, 2014; Lien et al. 2016). This event
111 has also expanded other components of the IGF system, including Igf1r (Alzaid et al. 2016a) and Igf-
112 II in some species (Lappin et al. 2016). Recent work on salmonid Igfbps in skeletal muscle has
113 included studies of *in vitro* regulation during myogenesis under anabolic and catabolic signals
114 (Gabillard et al. 2006; Bower and Johnston, 2010; Pooley et al. 2013) and *in vivo* regulation in
115 response to fasting (e.g. Bower et al., 2008), temperature (Hevrøy et al., 2013) and sex steroids
116 (Cleveland and Weber, 2015). Moreover, the salmonid Igfbp subtypes *igfbp1a1* and *igfbp6a2* have
117 roles linking salmonid growth to conserved cytokine pathways regulating inflammatory responses
118 (Alzaid et al. 2016b), with relevance to understanding muscle remodelling for energy reallocation
119 (Pooley et al. 2013). In contrast, the regulation of Igfbps by dexamethasone (or other glucocorticoids)
120 in fish skeletal muscle remains unstudied.
121
122 The objective of this study was to improve our understanding of how the Igfbp gene family is
123 regulated by a range of physiological stimuli known to induce remodelling of skeletal muscle mass.
124 We quantified the transcriptional responses of the complete repertoire of expressed Igfbps in primary
125 differentiated fast-twitch skeletal muscle cultures from Atlantic salmon (*Salmo salar* L.) using four
126 experimental models that induced a catabolic or anabolic status, via pathways regulated by
127 dexamethasone, proinflammatory cytokines, amino acids and Igf-I. Our results show distinct stimuli
128 result in divergent and complex expression responses of Igfbp family member genes during muscle
129 remodelling, including evolutionary divergence of salmonid-specific gene duplicates.
130

2. Materials and Methods

2.1. Ethics statement

The University of St Andrews Animal Ethics and Welfare Committee approved all the experimental procedures described. Fish were sacrificed by a blow to the head before sectioning of the spinal cord (Schedule-1 killing protocol; Animals Act 1986; Home Office Code of Practice. HMSO: London January 1997).

2.2. Myotube cell culture

Atlantic salmon (*Salmo salar* L.) were maintained at the Scottish Oceans Institute (University of St Andrews) in 200L fibreglass freshwater tanks at 10^{o}C with a 16:8 light/dark photoperiod. Myogenic progenitor cells (MPCs) were extracted from 10-14g Atlantic salmon parr (immature fish of unknown sex) and cell culture performed as previously described (Garcia de la serrana and Johnston, 2013). Briefly, epaxial fast skeletal muscle was extracted (total 40g of muscle, n=10 to 14 randomly-sampled fish per culture), mechanically dissected and enzymatically digested with trypsin and collagenase, then washed and filtered several times until MPCs were obtained. Cells were cultured in laminin-coated well plates and maintained with Dulbecco's modified eagle's media (DMEM; Sigma, Dorset, UK), 9mM NaHCO3 (pH 7.4) (Sigma), 20mM HEPES (Sigma), 10% (v/v) foetal bovine serum (Sigma) and an antibiotic/antimycotic cocktail (Sigma) at 18^{o}C for 10 days until fully differentiated myotubes were formed.

2.3. Experimental treatments

Catabolic and anabolic treatments were performed in day-10 differentiated Atlantic salmon myotubes in independent cultures (n=5). Catabolism was induced by addition of 1µM of dexamethasone (+DEX treatment) (Sigma), 3ng/ml of recombinant interleukin-1β (produced following Hong et al. 2001) (+IL-1β treatment) or using an amino acid free cell culture media (-AA treatment). In order to

157 establish conditions that induced myotube atrophy without affecting cell viability, dexamethasone
158 and IL-1β concentrations were obtained from the literature (Menconi et al., 2008; Pooley et al., 2013)
159 and a pilot study was carried out to test different concentrations (data not shown). Myotubes were
160 incubated in bovine serum free media for two hours to reduce gene expression to basal levels before
161 +DEX and +IL-1β treatments. Total RNA was extracted (section 2.4) at 0, 1, 3, 6, 24 and 48 hours
162 post-treatment. For the AA- treatment, a modified culture media with no amino acids was used
163 (Garcia de la serrana and Johnston, 2013) and total RNA extracted at 0, 1, 3, 6, 24 and 48 hours. The
164 anabolic treatment (+AA+Igf-I) involved a restitution of amino acids in the -AA cell culture media
165 (at 48 hours) combined with 100nM of recombinant Atlantic salmon Igf-I (GROPEP, Australia).
166 Total RNA from the +AA+Igf-I treatment was collected 3, 6 and 24 hours after the +AA+Igf-I
167 treatment. In all cases, myotubes with normal free-serum DMEM media were maintained in parallel
168 as controls (-DEX, -IL-1β, +AA and +AA-Igf-I) for each of the conditions tested and sampled at the
169 same time as treated cells.
170
171 **2.4. RNA extraction and cDNA synthesis**
172 Total RNA was extracted from two wells per time-point, per treatment and culture using an RNeasy
173 extraction kit (Qiagen, Manchester, UK), following the manufacturers protocol. RNA concentrations,
174 230/260 and 280/260 ratios were determined using a Nanodrop 1000 spectrophotometer (Nanodrop,
175 ThermoFisher Scientific). RNA with respective 260/280 and 260/280 ratios over 1.8 and 2 was used
176 for cDNA synthesis. 250ng of RNA was reverse transcribed for each sample using a Quantitech kit
177 (Qiagen), following the manufacturers guidelines, including a step to remove residual genomic DNA.
178 Control samples with RNA but no reverse transcriptase (-RT) were included. The 1:1 first-strand
179 cDNA was diluted 40x and stored at -20^{o}C until use in quantitative PCR (qPCR) (section 2.6). A pool
180 of all first-strand cDNAs generated was used as an interplate calibrator (IPC) for qPCR analysis
181 (section 2.6).
182

183 **2.5. Primer design**

184 Primers used for amplification of the complete salmonid Igfbp family (19 genes), as well as *mafbx*,
185 *murf1*, *igf2*, *myl1*, *tnni1* and the housekeeping genes *hprt1*, *rpl4*, *rps13*, *rps29* have been described
186 elsewhere (Bower et al., 2008; Macqueen et al., 2010; 2013; Alzaid et al., 2016b). New primers for
187 paralogues encoding autophagy related 4b cysteine protease (*atg4b*) genes were designed for use in
188 this study. First, BLASTn searches of the Atlantic salmon genome (via Salmobase.org) revealed two
189 *atg4b* paralogues on Chr. 10 and 16 (respective NCBI accession numbers: NM_001139775 and
190 XM_014149865), embedded within a large collinear duplicated block retained from the salmonid
191 specific WGD (Lien et al. 2016). These salmonid-specific paralogues were named *atg4b1* (Chr. 10)
192 and *atg4b2* (Chr. 16). Primers designed to be specific to each gene are as follows (underlined bases
193 distinguish the two paralogues): *atg4b1* - Fwd: 5' – GACTGGAGATGGGTGAGGAGC - 3'
194 (melting temperature, Tm = 61 ^{o}C); Rev: 5' – CCGTTAGGCTCTGGCATACC – 3' (Tm = 60 ^{o}C)
195 (product size = 382 bp) and *atg4b2* - Fwd: 5' – GAGACTGGAGATGGGTGAGAGG - 3' (Tm = 60
196 ^{o}C); Rev: 5' – GGCAGCCGTTATGCGTCG – 3' (Tm = 63 ^{o}C) (product size = 340 bp). For both
197 *atg4b* paralogues, the primers in a pair were separated by at least three exons in the gene.
198
199 **2.6. qPCR analysis**
200 All qPCR experiments were compliant with MIQE guidelines (Bustin et al., 2009). Each reaction
201 contained 6µl of 1:40-diluted cDNA, 7.5µl of 2x Brilliant III SYBRGreen master mix (Agilent,
202 Cheshire, UK) and 1.5µl of sense/antisense 500nM primer mix. Amplifications were performed in
203 duplicate in a Stratagene Mx3005P thermocycler (Agilent) with the following conditions: 3 min at
204 95^{o}C, followed by 40 cycles of 20s at 95^{o}C then 20s at 65^{o}C, followed by a dissociation analysis
205 (60°C to 95°C thermal gradient; single product observed in all final assays). No-template (-NT; water
206 in place of cDNA) and –RT controls were included in duplicate for each qPCR assay. The IPC cDNA
207 sample was included in quadruplicate using the same primer pair (*rps29*) on every qPCR plate.
208 Threshold crossing/quantification cycles (Cq) were calculated from baseline-corrected data with the

threshold fixed across plates at 0.25. Cq-36 was considered the cut-off of no expression (note: Cq was always >40 for -RT and -NTC controls). LinRegPCRv.11 software was used to calculate primer efficiency following the author's recommendations (Ruijter et al. 2009). Cq values were exported to Genex v.4.4.2 (MultiD Analyses AB) and corrected for differences in efficiency before any plate-to-plate variation was corrected using the IPC Cq values.

An assessment of reference gene suitability was performed using Normfinder (Andersen et al. 2004) within Genex. Normfinder was used to consider variance in expression of the four reference genes both globally and across the post-treatment time courses (considering controls vs. treatments). This was done with pooled cDNAs for each biological replicate (separate pools of replicates for +DEX, -DEX, +IL-1β, -IL-1β, –AA +AA, +AA+Igf1 and +AA-Igf1) and sampling points (0, 1, 3, 6, 24, and 48h) (n=42 sample points) providing a study-wide overview of reference gene stability. We also performed a Normfinder analysis of all four reference genes considering the Dexamethasone study with full biological replication (n=60 samples; -DEX and +DEX across 6 timepoints). Each of the four reference genes were expressed very stably in the pooled samples, both globally and with respect to treatment and time-point (Normfinder SD values: 0.17-0.22). The Dexamethasone data revealed that *rps29*, *rps13* and *rpl4* were stably expressed (global Normfinder SD values of 0.06-0.20), with *rps29* being the most stable. Importantly, the accumulative SD of references genes, which is indicative of the appropriate number of reference genes to employ for normalization, was not lowered (improved) by considering additional reference genes to *rps29*. Thus, using Genex, we normalized the efficiency-corrected Cq values for all experimental genes measured across the study to the relevant *rps29* Cq values, before placing the expression data on a relative scale quantitatively comparable across all experimental genes.

2.7. Muscle fibre diameter and immunofluorescence measurements

To measure myotube diameter and perform immunofluorescence detection, MPCs were grown on borosilicate coverslips coated with poly-L-lysine and laminin until fusion. Diameter was measured in 10-day differentiated myotubes from all tested treatments. Culture media was removed 24 and 48 hours after myotubes were incubated with the different treatments and control media, and washed twice with PBS. Duplicate coverslips for each time-point (24h and 48h; treatment and controls) were fixed in 4% (m/v) paraformaldehyde (Sigma) in PBS (pH 7.4) for 20 minutes at room temperature, washed twice with PBS and kept at 4°C in a solution of PBS 0.01% NaN_3 (Sigma) until further analysis. Photographs were taken at random for each time-point, treatment and culture (n=4 in each case), using a bright field microscope at 20x magnification. ImageJ software (National Institute of Health, Maryland, USA) was used to determine myotube diameter by measuring the thickness at 5 different locations along the myotube. Measurements were obtained from between 15 and 30 randomly selected myotubes. Final myotube diameter was taken as the average of the 5 measurements (100 to 150 myotubes per treatment/relevant controls).

Immunofluorescence against actin and desmin filaments was visualised based on a protocol outlined previously (Garcia de la serrana and Johnston, 2013). Fixed myotubes were washed twice in PBS and incubated with 0.5% Triton X-100 (v/v) (Sigma) PBS for 5 min. Non-specific binding sites were blocked with 5% (v/v) normal goat serum (Sigma), 1.5% (w/v) Bovine serum albumin (Sigma), 0.1% (v/v) Triton X-100 (v/v) PBS for 1 hour at room temperature. Actin filaments were visualized by incubation with Phalloidin-ATTO 488 antibody (Sigma) for 2 hours at room temperature at 1:100 dilution in 1.5% BSA (w/v) 0.1% Triton X-100 (v/v) PBS and counterstained with DAPI 1:500 in sterile water for 5 minutes. Desmin filaments were detected by incubating the cells with an anti-Desmin antibody (SIGMA) 1:20 (v/v) in 1.5% BSA 0.1% Triton X-100 PBS overnight at 4°C. To visualize the filaments, myotubes were incubated with anti-rabbit Alexa Fluor 546 (ThermoFisher) secondary antibody at 1:400 (v/v) dilution in 1.5% BSA 0.1% Triton X-100 for 2 hours at room temperature and counterstained with DAPI 1:500 in sterile water for 5 minutes. Myotubes were

visualized and digitally imaged using a Leica TCS SP2 confocal microscope (Leica Microsystems) at 20x magnification.

2.8. Statistical analysis

All statistical analyses were performed using RStudio (RStudio Team 2015). Pairwise comparisons of myotube diameter between treatments and controls were done using a Student's t-test. For analysis of the gene expression data, a general linear model approach was used with *treatment* and *time-point* as fixed factors. The Shapiro-Wilk test was used to scrutinize the assumption of normality in the linear model residuals. Expression data that failed to follow a normal distribution was transformed using a Box-Cox power transformation and tested again. Data that did not follow normality after Box-Cox power transformation was analysed using a Kruskal-Wallis non-parametric test.

3. Results

3.1. Effect of catabolic and anabolic treatments on myotube diameter

The effect of the different treatments on salmon myotube morphology and cytoskeleton arrangement was assessed 24 and 48 hours after treatment using bright field microscopy and immunofluorescence against actin and desmin filaments (Figure 1A; Supplementary File 1). After 48 hours treatment, each tested catabolic treatment caused a reduction in the number of differentiated myotubes and an increase in the presence of single cells, evidenced both by bright microscopy (Figure 1A, i-k vs. control data in a-c) and desmin immunofluorescence (Figure 1A, m-o vs. control data in e-g). Considering that we used differentiated myotubes as the starting point for each treatment, a reduction in the number of myotubes, coupled with an increase in the number of single cells, might be explained by a dramatic reduction in the integrity of the myotube cytoskeleton. In other words, the apparent single cells may actually remain part of myotubes where the cytoskeleton has undergone extensive atrophy. Bright-field microscopy (Figure 1A, d, i) and desmin immunofluorescence (Figure

1A, h, p) showed that the addition of amino acids and Igf-I (+AA+Igf) to myotubes under amino acid deprivation for 48h (-AA-48h) (Figure 1A, d, h) induced myotube hypertrophy (Figure 1A, i, p).

To quantify the accompanying phenotypic changes in myotubes, we compared myotube diameters for all treatments against controls. +DEX and -AA treatments reduced myotube diameter by ~30-40% at 24 and 48 hours compared to controls (all $P < 0.001$) (Figure 1B and C). The +IL-1β treatment reduced myotube diameter by ~10% at 24 hours ($P = 0.055$) and by ~30% at 48 hours ($P < 0.001$) (Figure 1D). When amino acids and Igf-I were added to the -AA culture (-48h time-point), myotube diameter increased to pre-treatment values in 24h ($P < 0.001$) (Figure 1B). These data confirm that the treatments induced the intended myotube phenotypic changes, which provides a robust platform to interpret gene expression responses measured in the same experimental samples (section 3.2).

3.2. Gene expression responses to catabolic and anabolic stimuli

Genes encoding all 19 Igfbps were quantified using qPCR in Atlantic salmon myotubes, but 10 were not detected, namely *igfbp1a2*, *igfbp1b1*, *igfbp2b1*, *igfbp2b2*, *igfbp3a2*, *igfbp3b1*, *igfbp3b2*, *igfbp6a2* and *igfbp6b1*. Given that the relevant primers have been verified in past studies where expression of all 19 genes was reported (e.g. Macqueen et al. 2013; Alzaid et al. 2016b), we concluded that these *igfbp* genes were not expressed in salmon myotubes. In parallel, genes encoding two E3-ubiquitin ligases (*mafbx*, *murf1*), two fast-twitch skeletal muscle sarcomere components (myosin light chain, *myl1* and troponin I, *tnni1*), the Igf-II hormone (*igf2*) and two autophagy related genes (*atg4b1*, *atg4b2*) were also analysed.

3.2.1. +DEX treatment

10 of the 16 tested genes were significantly regulated by the +DEX treatment compared to controls ($P <0.05$ for *treatment* effect), including those encoding 6 of the 10 expressed Igfbp family members, both tested E3 Ubiquitin ligases, one of the *atg4b* paralogues and *igf2* (Table 1). In addition, 4 of the

10 genes with a significant treatment effect showed a significant *treatment*time-point* interaction, indicating marked differences in the response to dexamethasone at different time-points (Table 1). Among these were two genes encoding Igfbp6 family members (*igfbp6a1* and *igfbp6b2*), which showed reciprocal responses across the treatment time course. Specifically, comparing +DEX to control cultures, *igfbp6a1* was most highly downregulated, while *igfbp6b2* was most highly upregulated at later time-points (24 to 48 hours) of the culture (Figure 2A, B), where atrophy was evident (Figure 1B-D). A similar pattern was observed for two Igfbp5 family members, with *igfbp5a* being downregulated at 24 to 48 hours post treatment and *igfbp5b1* being strongly induced from 6 hours post-treatment (Figure 2C, D). The other two Igfbp family members that responded significantly to the +DEX treatment (*igfbp4* and *igfbp2a*) showed a less pronounced trend in the nature and magnitude of response across time-points (Figure 2E, F). The two E3 Ubiquitin ligase genes showed highly distinct responses to the +DEX treatment (Figure 2G, H). Specifically, *mafbx* was induced from early stages of the culture (before notable changes in myotube diameter were observed), through to 24 hours, when atrophy was first observed (Figure 1C) but returned to control levels by 48 hours (Figure 2G). Conversely, *murf1* was induced relative to control levels at 24 and 48 hours sampling points (Figure 2H). In addition, both *igf2* and *atgb42* were markedly induced at 24 and 48 hours post +DEX treatment (Figure 2I, H).

Therefore, the most pronounced changes in gene expression responses to dexamethasone occurred at stages of the culture (post-6 hours), when myotube remodelling was evident.

3.2.3. +IL-1β treatment

Despite our observation that myotube diameter decreased significantly in response to the +IL-1β treatment by 48 hours (Figure 1D), only 2 of the 16 tested genes were significantly regulated during this remodelling of myotube phenotype (Table 2; Figure 3). This included *igfbp1a1*, which was

downregulated at 3, 6 and 48 hours post-treatment, but not other time-points (Table 2; Figure 3A). In contrast, *murf1* was increased in response to controls, most notably at 48 hours (Figure 3B).

3.2.4. -AA treatment

The -AA treatment was accompanied by significant responses in only 3 of the 16 tested genes (Table 3; Figure 4), despite clear evidence of myotube atrophy (Figure 1B). Two of the genes significantly regulated by the –AA treatment were the same Igfbp6 family members that were strongly affected by dexamethasone (section 3.2.2). Specifically, both *igfbp6a1* and *igfbp6b2* were downregulated during the –AA treatment time course relative to controls (Table 3), with *igfbp6a1* being particularly strongly affected from 6 hours post treatment (Figure 4A, B). The other gene significantly affected by the –AA treatment, *mafbx*, was downregulated at many sampled time-points (Table 3; Figure 4C).

3.2.5. +AA+Igf-I treatment

The +AA+Igf-I treatment, which was accompanied by a significant recovery of myotube diameter (i.e. anabolic state) (Figure 1B), led to significant responses in 8 of the 16 tested genes, including 4 encoding Igfbp family members, *mafbx*, *igf2* and both paralogues of *atg4b* (Table 4; Figure 5). Among the significantly responsive Igfbp genes, three were increased, either transiently (*igfbp6b2*, Figure 5A), or consistently across multiple timepoints (*igfbp5b1* and *igfbp4*, Figure 5B, C). Conversely, *igfbp1a1* was downregulated at all timepoints post +AA+Igf-I treatment (Figure 5D). Finally, while *mafbx* and both *atgb4b* duplicates were downregulated by the +AA+Igf-I treatment at multiple sampled timepoints, *igf2* was upregulated (Figure 5E-H).

4. Discussion

Here we addressed the regulation of Igfbp gene expression in skeletal muscle remodelling, which is poorly understood in teleost fish. Our study is the first to systematically document the regulation of

364 the complete Igfbp gene family under several distinct catabolic and anabolic conditions, done with
365 full knowledge of gene paralogues retained from both the teleost and salmonid-specific WGD events,
366 which if ignored can limit physiological interpretations of gene expression (Johnston et al. 2011).
367 Though all three tested catabolic signals (i.e. dexamethasone, IL-1β and amino acid deprivation)
368 induced atrophy of differentiated myotubes (Figure 1), the responses of different Igfbp genes, as well
369 as other relevant marker genes, showed remarkable variability across the tested experimental models
370 (Tables 1-3; Figures 2-5). This was true not only for the number of genes showing a significant
371 response (i.e. from only 2 genes responding to IL-1β, up to 10 to dexamethasone), but also the
372 particular Igfbp genes that responded to different stimuli. This points to complex and context-
373 dependent transcriptional regulation of Igfbp gene expression via several unique pathways that
374 promote muscle remodelling.
375
376 Dexamethasone-induced atrophy of salmon myotubes (Figure 1) was accompanied by a complex
377 expression response of different Igfbp genes (Figure 2). The catabolic state of the myotubes was also
378 evidenced by upregulation of *mafbx, murf1* and *atg4b1* (Table 1), suggesting activation of the
379 proteasome and autophagy systems. However, we also observed Igf system expression responses that
380 are difficult to reconcile with a purely catabolic state, particularly the upregulation of *igf2*, *igfbp4* and
381 *igfbp5b1* (Table 1). While past work has showed that *igf2* is likewise induced by dexamethasone in
382 salmonid hepatocytes (Pierce et al. 2010), its protein product, along with Igfbp5, are established pro-
383 myogenic factors in mammals with key roles in differentiation (e.g. Stewart et al. 1996; Ren et al.
384 2008). Similarly, *igfbp4* has pro-growth functions in salmonid muscle (Johnston et al. 2011; e.g.
385 Bower et al. 2008; Macqueen et al. 2011). Despite this, past *in vitro* studies have also shown that both
386 *igf2* and *igfbp5b1* are much more highly expressed in mononuclear MPCs compared to differentiated
387 myotubes, suggesting roles in early phases of myogenesis, such as MPC proliferation (Bower and
388 Johnston, 2010). Additionally, dexamethasone, despite being a potent inducer of atrophy (e.g. Braun
389 and Marks, 2015) has been shown to activate IGF-signalling pathways promoting early phases of

myogenesis (Giorgino and Smith, 1995). Thus, some observed Igfbp system expression responses might result from stimulation of such IGF-signalling pathways, despite the overall catabolic status of salmon myotubes.

The reciprocal responses of two functionally-related Igfbp5 teleost family members to dexamethasone, with *igfbp5a* downregulated and *igfbp5b1* upregulated (Figure 2C, D) is also notable, as past reports have suggested that mammalian Igfbp5, while being essential for mammalian muscle differentiation (Ren et al. 2008), can also inhibit muscle differentiation under some physiological contexts (Ewton et al. 1998). One explanation for our data is that such divergent roles of Igfbp5 have been partitioned to the individual teleost paralogues during evolution. Interestingly, among the other Igfbp genes that responded to dexamethasone, only *igfbp6a1* and *igfbp6b2* were significantly regulated under any other tested atrophy stimulus, specifically in response to amino acid deprivation (discussed further below). Even then, while *igfbp6a1* was downregulated under both conditions, consistent with a common underlying role, *igfbp6b2* was upregulated by dexamethasone, but downregulated by amino acid deprivation. Moreover, during recovery myotube growth (induced by addition of amino acids and Igf-I to cell cultures previously deprived of amino acids), *igfbp6b2* was increased (i.e. as observed for dexamethasone) despite the myotube showing an anabolic rather than catabolic status. The role of Igfbp6 in teleost muscle remodelling is clearly complex (discussed below), both in response to dexamethasone and other signals, and warrants further study.

In contrast to dexamethasone, IL-1β-induced myotube atrophy was not accompanied by marked changes in the expression of Igfbp family members and other tested genes (Table 2). This contrasts two past studies where a much higher dose of IL-1β was administered to Atlantic salmon myocytes previously cultured for 4 days (25 ng/ml dose; Pooley et al. 2013) or 7 days (50-200 ng/ml dose; Heidari et al. 2016) and several Igfbp genes were strongly affected (Pooley et al. 2013), including the robust induction of an undefined Igfbp6 family member (Pooley et al. 2013; Heidari et al. 2016).

416 However, as we cultured myocytes for 10 days before IL-1β treatment, our study represents a more
417 advanced state of differentiation (Bower et al., 2010; Bower and Johnston, 2010; Garcia de la serrana
418 et al., 2013). Thus, the discrepancies between our study and these past investigations presumably
419 reflect differences in both the concentrations of IL-1β used, but potentially also the ontogeny of the
420 cell culture. Interestingly, in another study, a strong upregulation of *Igfbp6a2* was observed in
421 rainbow trout (*Oncorhynchus mykiss*) following *in vivo* bacterial challenge at the fry stage, a response
422 that was strikingly correlated to that of master genes regulated by proinflammatory cytokine
423 pathways, including *IL-1β* (Alzaid et al. 2016b). However, in that past study, the tissues responsible
424 for *igfbp6a2* upregulation were not determined and whether skeletal muscle was involved remains
425 unknown. In our study, *igfbp1a2* (the single Igfbp1 family member expressed in myotubes) was
426 slightly downregulated in response to IL-1β (Table 2). However, its salmonid-specific paralogue
427 *igfbp1a2* is robustly induced during bacterial infection, which is presumed to restrict Igf hormones in
428 the circulation (Alzaid et al. 2016b), consistent with past studies showing that salmonid Igfbp1 family
429 members are upregulated in circulation in response to catabolic physiological states (e.g. Kawaguchi
430 et al. 2015). Thus, the downregulation of *igfbp1a2* in atrophic salmon myotubes points to differences
431 in the local and systematic roles of Igfbp1 family members of teleosts. In addition, past work
432 documented a minor induction of *mafbx* in response to IL-1β in salmon myocytes (Pooley et al.
433 2013), which, again was not detected in our study. However, *murf1*, another E3-Ubiquitin ligase, was
434 upregulated (Table 2). Past reports in mammal myotubes has shown that both E3-Ubiquitin ligases
435 are stimulated by IL-1β through NF-κB signalling pathways (e.g. Li et al. 2009).
436
437 As for IL-1β, we observed a paucity of transcriptional responses in atrophic salmon myotubes
438 deprived of amino acids (Table 3), similar to previous reports (Bower and Johnston, 2010). However,
439 a separate past study showed that the E3-Ubiquitin ligase *mafbx* was robustly induced by the same
440 treatment (Bower et al. 2010), which was not observed in our data. The only other genes that
441 responded to amino acid deprivation were *igfbp6a1* and *igfbp6b2* (Figure 4A, B), which were each

strongly decreased, which contrasts with the fact that Igfbp6 is a negative regulator of Igf signalling, particularly through Igf-II, which in mammals binds Igfbp6 with much higher affinity than Igf-I (Bach, 2016). Thus, we suggest that the complex expression responses of different Igfbp6 family members observed in our study, with both positive and negative regulation in myotubes under verified catabolic states is likely related to the plethora of characterized cellular actions for Igfbp6 that are IGF-independent (Bach, 2016).

A stronger expression response for the tested genes was observed during myotube recovery growth induced by amino acids and Igf-I treatment in previously-fasted salmon myotubes, including downregulation of *mafbx* and both *atg4b* paralogues, suggesting repression of the proteasome and autophagy pathways. A concurrent upregulation of several Igf system genes that are considered pro-myogenic, including *igf2*, *igfbp5b1* and *igfbp4*, was also consistent with the observed anabolic state of myotubes and highly congruent with past data using a similar experimental model (Bower et al., 2008). However, the strong episodic upregulation of *igfbp6b2* in response to the +AA+Igf-I treatment (Figure 6A) has not been observed before and will warrant further investigation, especially in light of the diverse expression responses of Igfbp6 family members observed in our broader study.

A final discussion point is the differential expression of salmonid-specific paralogues in our study. Past work has emphasized the enormous extent of transcriptional divergence that has evolved among such duplicates since the salmonid WGD ~95 Ma, which has been previously demonstrated both at the genome-wide level (across tissues; Lien et al. 2016) and for important gene families in response to various physiological stimuli (e.g. Macqueen et al. 2010; Garcia de la Serrana et al. 2013; Alzaid et al. 2016b). For the Igfbp family, the only such gene duplicates expressed in salmon myotubes were *igfbp5b1* and *igfbp5b2*. In a recent past study, these two genes were shown to have similar regulation during the early development of rainbow trout (Alzaid et al. 2016b). Here, we observed divergent responses of *igfbp5b1* and *igfbp5b2* to dexamethasone (Table 1) and the +AA+Igf-1 treatment (Table

468 4), which likely reflects evolutionary divergence in regulatory sequences controlling transcription.
469 Again, such findings emphasize the importance of identifying and distinguishing gene duplicates in
470 investigations of salmonid physiology.
471
472 **5. Conclusion**
473 This study improves our understanding about how a range of stimuli induce catabolic and anabolic
474 status in salmonid myotubes and highlights great evident complexity in the roles played by different
475 Igfbp family members in the control of salmonid skeletal muscle mass.
476
477 **6. Acknowledgements**
478 This work received funding from the MASTS pooling initiative (The Marine Alliance for Science
479 and Technology for Scotland) and their support is gratefully acknowledged. MASTS is funded by the
480 Scottish Funding Council (grant reference HR09011) and contributing institutions.
481
482 **7. Declaration of Interest**
483 The authors declare that they have no competing interests.
484
485 **References**
486
487 Alzaid, A., Martin, S.A., Macqueen, D.J. 2016a. The complete salmonid IGF-IR gene repertoire and
488 its transcriptional response to disease. Sci Rep. 6, 34806.
489
490 Alzaid, A., Castro, R., Wang, T., Secombes, C.J., Boudinot, P., Macqueen, D.J., Martin, S.A. 2016b.
491 Cross-talk between growth and immunity: coupling of the insulin-like growth factor axis to
492 conserved cytokine pathways in rainbow trout. Endocrinology. 157, 1942-55.
493

494 Andersen, C.L., Jensen, J.L., Orntoft, T.F. 2004. Normalization of real-time quantitative reverse
495 transcription-PCR data: a model-based variance estimation approach to identify genes suited for
496 normalization, applied to bladder and colon cancer data sets. Cancer Res. 64, 5245-50.
497
498 Bach, L.A. 2016. Current ideas on the biology of IGFBP-6: More than an IGF-II inhibitor? Growth
499 Horm IGF Res. *In press*, pii: S1096-6374(16)30056-9.
500
501 Bonaldo, P. and Sandri, M. 2013. Cellular and molecular mechanisms of muscle atrophy. Dis Model
502 Mech. 6, 25-39.
503
504 Bower, N.I., Li, X., Taylor, R., Johnston, I.A. 2008. Switching to fast growth: the insulin-like growth
505 factor (IGF) system in skeletal muscle of Atlantic salmon. J. Exp Biol. 211, 3859-3870.
506
507 Bower, N.I. and Johnston, I.A. 2010. Transcriptional regulation of the IGF signaling pathway by
508 amino acids and insulin-like growth factors during myogenesis in Atlantic salmon. PLoS One. 5,
509 e11100.
510
511 Bower N.I., Garcia de la Serrana, D., Johnston, I.A. 2010. Characterisation and differential regulation
512 of MAFbx/Atrogin-1 alpha and beta transcripts in skeletal muscle of Atlantic salmon (*Salmo salar*).
513 Biochem Biophys Res Commun. 396, 265-71.
514
515 Bustin, S.A., Benes, V., Garson, J.A., Hellemans, J., Huggett, J., Kubista, M., Mueller, R., et al.
516 2009. The MIQE guidelines: minimum information for publication of quantitative real-time PCR
517 experiments. Clin Chem. 55, 611-22.
518

519 Braun, T.P. and Marks, D.L. 2015. The regulation of muscle mass by endogenous glucocorticoids.
520 Front Physiol. 3, 6-12.
521
522 Calnan, D. R. and Brunet, A. 2008. The FoxO code. Oncogene 27, 2276–2288.
523
524 Cleveland, B.M. and Weber, G.M. 2015. Effects of sex steroids on expression of genes regulating
525 growth-related mechanisms in rainbow trout (*Oncorhynchus mykiss*). Gen Comp Endocrinol.
526 216,103-15.
527
528 Duan, C. and Xu, Q. 2005. Roles of insulin-like growth factor (IGF) binding proteins in regulating
529 IGF actions. Gen Comp Endocrinol. 142, 44-52.
530
531 Duan, C., Ren, H., Gao, S. 2010. Insulin-like growth factors (IGFs), IGF receptors, and IGF-binding
532 proteins: roles in skeletal muscle growth and differentiation. Gen Comp Endocrinol. 167, 344-51.
533
534 Ewton, D.Z., Coolican, S.A., Mohan, S., Chernausek, S.D., Florini, J.R. 1998. Modulation of insulin-
535 like growth factor actions in L6A1 myoblasts by insulin-like growth factor binding protein (IGFBP)-
536 4 and IGFBP-5: a dual role for IGFBP-5. J Cell Physiol. 177, 47-57.
537
538 Firth, S.M. and Baxter, R.C. 2002. Cellular actions of the insulin-like growth factor binding proteins.
539 Endocr Rev. 23, 824-54.
540
541 Gabillard, J.C., Kamangar, B.B., Montserrat, N. 2006. Coordinated regulation of the GH/IGF system
542 genes during refeeding in rainbow trout (*Oncorhynchus mykiss*). J Endocrinol. 191, 15-24.
543

544 Garcia de la serrana, D. and Johnston, I.A. 2013. Expression of heat shock protein 90 (Hsp90)
545 paralogues is regulated by amino acids in skeletal muscle of Atlantic salmon. PLoS ONE. 8, e74295.
546
547 Giorgino, F. and Smith, R.J. 1995. Dexamethasone enhances insulin-like growth factor-I effects on
548 skeletal muscle cell proliferation. Role of specific intracellular signaling pathways. J Clin Invest. 96,
549 1473-83.
550
551 Glass, D.J. 2005. Skeletal muscle hypertrophy and atrophy signaling pathways. Int J Biochem Cell
552 Biol. 37, 1974-84.
553
554 Heidari, Z., Bickerdike, R., Tinsley, J., Zou, J., Wang, T.Y., Chen, T.Y., Martin, S.A. 2016.
555 Regulatory factors controlling muscle mass: competition between innate immune function and
556 anabolic signals in regulation of atrogin-1 in Atlantic salmon. Mol Immunol. 67, 341-9.
557
558 Hers, I., Vincent, E.E., Tavaré J.M. 2011. Akt signalling in health and disease. Cell Signal. 23, 1515-
559 27.
560
561 Hevrøy, E.M., Hunskår, C., de Gelder, S., Shimizu, M., Waagbø, R., Breck, O., Takle, H., et al. 2013.
562 GH-IGF system regulation of attenuated muscle growth and lipolysis in Atlantic salmon reared at
563 elevated sea temperatures. J Comp Physiol B. 183, 243-59.
564
565 Hong, S., Zou, J., Crampe, M., Peddie, S., Scapigliati, G., Bols, N., Cunningham, C., et al. 2001. The
566 production and bioactivity of rainbow trout (*Oncorhynchus mykiss*) recombinant IL-1 beta. Vet
567 Immunol Immunopathol. 81, 1-14.
568

James, R.S. and Johnston I.A. 1998. Influence of spawning on swimming performance and muscle contractile properties in the short-horn sculpin. J Fish Biol. 53, 485-501.

Johnston, I.A., Bower, N.I., Macqueen, D.J. 2011. Growth and the regulation of myotomal muscle mass in teleost fish. J Exp Biol. 214, 1617-1628.

Kawaguchi, K., Kaneko, N., Fukuda, M., Nakano, Y., Kimura, S., Hara, A., Shimizu, M. 2015. Responses of insulin-like growth factor (IGF)-I and two IGF-binding protein-1 subtypes to fasting and re-feeding, and their relationships with individual growth rates in yearling masu salmon (*Oncorhynchus masou*). Comp Biochem Physiol A Mol Integr Physiol. 165, 191-8

Laron, Z. 1996. The somatostatin-GHRH-GH-IGF axis. In: Merimee T, Laron Z eds. Growth hormone, IGF-I and growth: new views of old concepts. Modern endocrinology and diabetes, Vol. 4. London-Tel Aviv: Freund Publishing House Ltd. Pp 5–10.

Lappin, F.M., Shaw, R.L., Macqueen, D.J. 2016. Targeted sequencing for high-resolution evolutionary analyses following genome duplication in salmonid fish: Proof of concept for key components of the insulin-like growth factor axis. Mar Genomics. *In press*, doi: 10.1016/j.margen.2016.06.003.

Li, W., Moylan, J.S., Chambers, M.A., Smith, J., Reid, M.B. 2009. Interleukin-1 stimulates catabolism in C2C12 myotubes. Am J Physiol Cell Physiol. 297, C706-14.

Lien, S., Koop, B.F., Sandve, S.R., Miller, J.R., Kent, M.P., Nome, T., Hvidsten, T.R., et al. 2016. The Atlantic salmon genome provides insights into rediploidization. Nature. 533, 200-5.

595 Macqueen, D.J., Kristjánsson, B.K., Johnston, I.A. 2010. Salmonid genomes have a remarkably
596 expanded akirin family, coexpressed with genes from conserved pathways governing skeletal muscle
597 growth and catabolism. Physiol Genomics. 42, 134-48.
598
599 Macqueen, D.J., Kristjánsson, B.K., Paxton, C.G., Vieira, V.L., Johnston, I.A. 2011. The parallel
600 evolution of dwarfism in Arctic charr is accompanied by adaptive divergence in mTOR-pathway
601 gene expression. Mol Ecol. 20, 3167-84.
602
603 Macqueen, D.J., Garcia de la serrana, D., Johnston, I.A. 2013. Evolution of ancient functions in the
604 vertebrate insulin-like growth factor system uncovered by study of duplicated salmonid fish genomes.
605 Mol Biol Evol. 30, 1060-76.
606
607 Macqueen, D.J. and Johnston, I.A. 2014. A well-constrained estimate for the timing of the salmonid
608 whole genome duplication reveals major decoupling from species diversification. Proc Biol Sci. 281,
609 1778.
610
611 Macqueen, D.J., Fuentes, E.N., Valdés, J.A., Molina, A., Martin, S.A. 2014. The vertebrate muscle-
612 specific RING finger protein family includes MuRF4--a novel, conserved E3-ubiquitin ligase. FEBS
613 Lett. 588, 4390-7.
614
615 Mammucari, C., Milan, G., Romanello, V., Masiero, E., Rudolf, R., Del Piccolo, P., Burden, S.J., et
616 al. 2007. FoxO3 controls autophagy in skeletal muscle in vivo. Cell Metab. 6, 458-71.
617
618 Menconi, M., Gonnella, P., Petkova, V., Lecker, S., Hasselgren, P.O. 2008. Dexamethasone and
619 corticosterone induce similar, but not identical, muscle wasting responses in cultured L6 and C2C12
620 myotubes. J Cell Biochem.105, 353-64.

621

622 Mommsen, T.P. 2004. Salmon spawning migration and muscle protein metabolism: the August
623 Krogh principle at work. Comp Biochem Physiol B Biochem. Mol Biol. 139: 383-400.

624

625 Murton, A.J., Constantin, D., Greenhaff, P.L. 2008. The involvement of the ubiquitin proteasome
626 system in human skeletal muscle remodelling and atrophy. Biochim Biophys Acta.1782, 730-43.

627

628 Ocampo Daza, D., Sundström, G., Bergqvist, C.A., Duan, C., Larhammar, D. 2011. Evolution of the
629 insulin-like growth factor binding protein (IGFBP) family. Endocrinology. 152, 2278-89.

630

631 Pierce, A.L., Dickey, J.T., Felli, J., Swanson, P., Dickhoff, W.W. 2010. Metabolic hormones regulate
632 basal and growth hormone-dependent igf2 mRNA level in primary cultured coho salmon
633 hepatocytes: effects of insulin, glucagon, dexamethasone, and triiodothyronine. J Endocrinol. 204,
634 331-9.

635

636 Pooley, N.J., Tacchi, L., Secombes, C.J., Martin, S.A. 2013. Inflammatory responses in primary
637 muscle cell cultures in Atlantic salmon (*Salmo salar*). BMC Genomics. 14, 747.

638

639 Ren, H., Yin, P., Duan C. 2008. IGFBP-5 regulates muscle cell differentiation by binding to IGF-II
640 and switching on the IGF-II auto-regulation loop. J Cell Biol. 182, 979-91.

641

642 RStudio Team. 2015. RStudio: Integrated Development for R. RStudio, Inc., Boston, MA.
643 http;//ww.rstudio.com/

644

Ruijter, J.M., Ramakers, C., Hoogaars, W., Bakker, O., van den Hoff, M.J.B., Karlen, Y., Moorman, A.F.M. 2009. Amplification efficiency: linking baseline and bias in the analysis of quantitative PCR data. Nucleic Acids Res. 37, e45.

Sacheck, J.M., Hyatt, J.P., Raffaello, A., Jagoe, R.T., Edgerton, V.R., Lecker, S.H., Goldberg, A.L. 2007. Rapid disuse and denervation atrophy involve transcriptional changes similar to those of muscle wasting during systemic diseases. FASEB J. 21, 140-55.

Sandri, M., Sandri, C., Gilbert, A., Skurk, C., Calabria, E., Picard, A., Walsh, K., et al. 2004. Foxo transcription factors induce the atrophy-related ubiquitin ligase atrogin-1 and cause skeletal muscle atrophy. Cell. 117, 399-412.

Schiaffino, S. and Mammucari, C., 2011. Regulation of skeletal muscle growth by the IGF1-Akt/PKB pathway: insights from genetic models. Skelet Muscle. 4, 18.

Schiaffino, S., Dyar, K.A., Ciciliot, S., Blaauw, B., Sandri, M. 2013. Mechanisms regulating skeletal muscle growth and atrophy. FEBS J. 280, 4294-4314.

Seiliez, I., Gutierrez, J., Salmerón, C., Skiba-Cassy, S., Chauvin, C., Dias, K., Kaushik, S., et al. 2010. An in vivo and in vitro assessment of autophagy-related gene expression in muscle of rainbow trout (*Oncorhynchus mykiss*). Comp Biochem Physiol B Biochem Mol Biol. 157, 258-66

Shimizu, N., Yoshikawa, N., Ito, N., Maruyama, T., Suzuki, Y., Takeda, S., Nakae, J., et al. 2011. Crosstalk between glucocorticoid receptor and nutritional sensor mTOR in skeletal muscle. Cell Metab. 13, 170–182.

671 Southgate, R.J., Neil, B., Prelovsek, O., El-Osta, A., Kamei, Y., Miura, S., Ezaki, O., et al. 2007.
672 FOXO1 regulates the expression of 4E-BP1 and inhibits mTOR signaling in mammalian skeletal
673 muscle. J Biol Chem. 282, 21176–21186.
674
675 Stewart, C.E., James, P.L., Fant, M.E., Rotwein, P. 1996. Overexpression of insulin-like growth
676 factor-II induces accelerated myoblast differentiation. J Cell Physiol. 169, 23–32.
677
678 Tzivion, G., Dobson, M., Ramakrishnan, G. 2011. FoxO transcription factors; Regulation by AKT
679 and 14-3-3 proteins. Biochim Biophys Acta. 1813, 1938-45.
680
681 Wang, X. and Proud, C.G. 2006. The mTOR pathway in the control of protein synthesis. Physiology
682 (Bethesda). 21, 362-9.
683
684 Wood, A.W., Duan, C., Bern, H.A. 2005. Insulin-like growth factor signaling in fish. Int Rev Cytol.
685 243, 215–285.
686
687
688
689
690
691
692
693
694
695
696

Figure legends

Figure 1. Changes in Atlantic salmon myotubes in response to catabolic and anabolic treatments. (**A**) Bright field images (a-d, i-l) or immunofluorescence against desmin filaments (e-h, m-p) is shown in response to the +IL-1β (a, e, i, m), -AA (b, f, j, n), +DEX (c, g, k, o) and +AA+Igf-I (d, h, l, p) treatments after 48 hours. All pictures were taken at 20x magnification. The scale bars represent 150µm. (**B**) Changes in myotube diameter in response to -AA treatment vs. controls (+AA) and +AA+IGF treatment. (**C**) Changes in myotube diameter in response to the +DEX treatment vs. controls (-DEX). (**D**) Changes in myotube diameter in response to +IL-1β treatment vs. controls (-IL-1β). Each box and whisker plot shows measurements from 100 to 150 myotubes. Significant differences ($P < 0.05$) between controls and treatments are indicated at 24 hours (*), 48 hours (#) and between -AA vs. +AA+IGF (+). The symbols '***', '###' and '+++' highlight differences at $P < 0.001$.

Figure 2. Significant mRNA-level expression responses to +DEX treatment for *igfbp6a1* (**A**), *igfbp6b2* (**B**), *igfbp5a* (**C**), *igfbp5b1* (**D**), *igfbp4* (**E**), *igfbp2a* (**F**), *mafbx* (**G**), *murf1* (**H**), *igf2* (**I**) and *atg4b2* (**J**) at 0, 1, 3, 6, 24 and 48 hours post-treatment showed as arbitrary units for controls (full bar chart) and treated (empty bar chart) myotubes. Values for bar chart are mean + SD (n=5). Complete details of gene expression responses for all genes tested in the study is provided in Table 1.

Figure 3. Significant mRNA-level expression responses to +IL-1β treatment for *igfbp1a1* (**A**) and *murf1* (**B**). All other details are as given in the Figure 2 legend. Complete details of gene expression responses for all genes tested in the study is provided in Table 2.

Figure 4. Significant mRNA-level expression responses to –AA treatment for *igfbp6a1* (**A**), *igfbp6b2* (**B**) and *mafbx* (**C**). All other details are as given in the Figure 2 legend. Complete details of gene expression responses for all genes tested in the study is provided in Table 3.

723

724 **Figure 5**. Significant mRNA-level expression responses to +AA+Igf-I treatment for *igfbp6b2* (**A**),
725 *igfbp5b1* (**B**), *igfbp4* (**C**), *igfbp1a1* (**D**), *mafbx* (**E**), *igf2* (**F**), *atg4b1* (**G**) and *atg4b2* (**H**) at 3, 6 and 24
726 hours post-treatment. All other details are as given in the Figure 2 legend. Complete details of gene
727 expression responses for all genes tested in the study is provided in Table 4.

728

729 **Supplementary File 1**. Myotube morphology in response to catabolic and anabolic treatments.
730 Bright field microscopy or immunofluorescence against desmin (red) and actin (green) filaments for
731 myotubes under different experimental conditions. All pictures were taken using x20 magnification.
732 The scale bar for each picture represents 150µm.

733

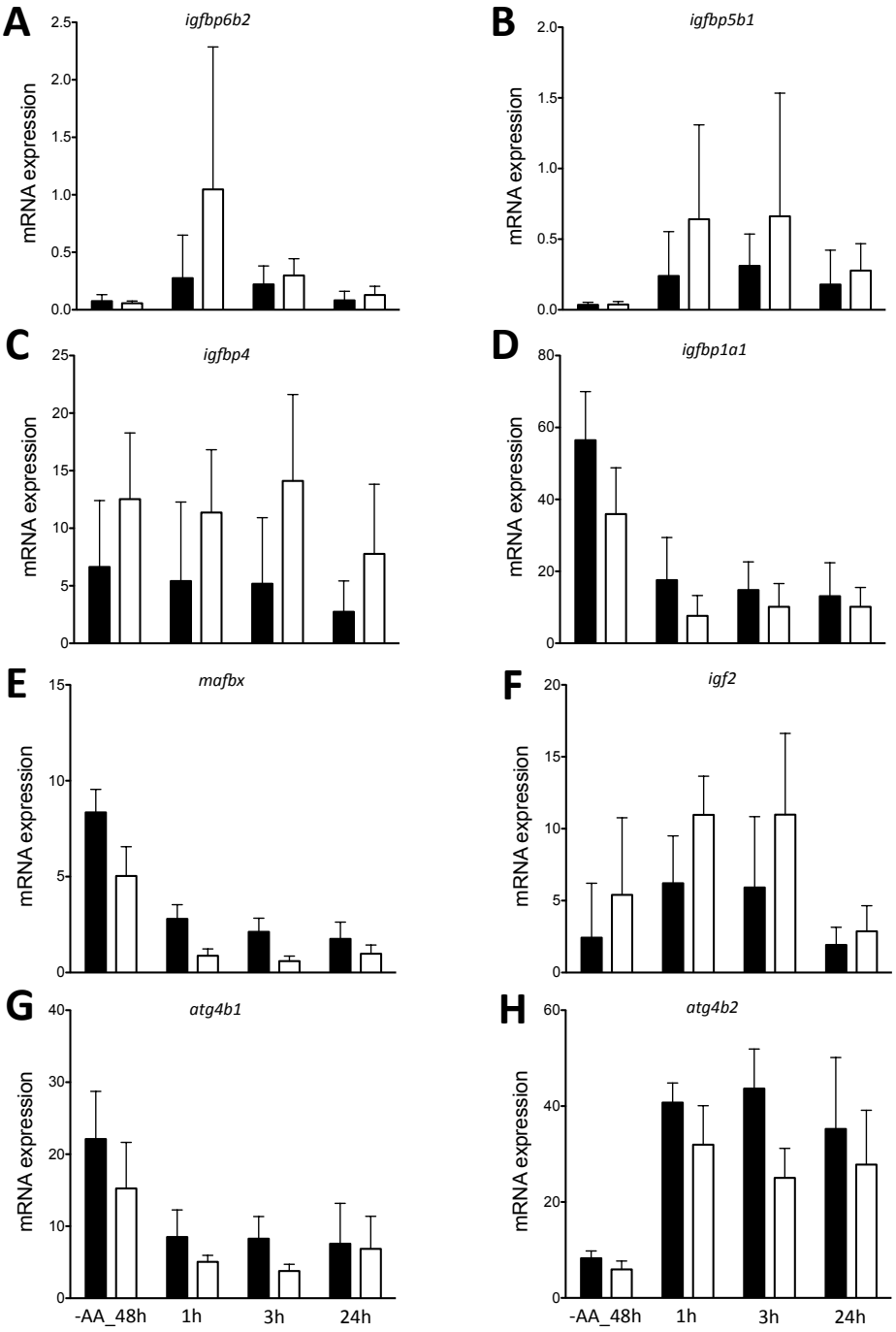

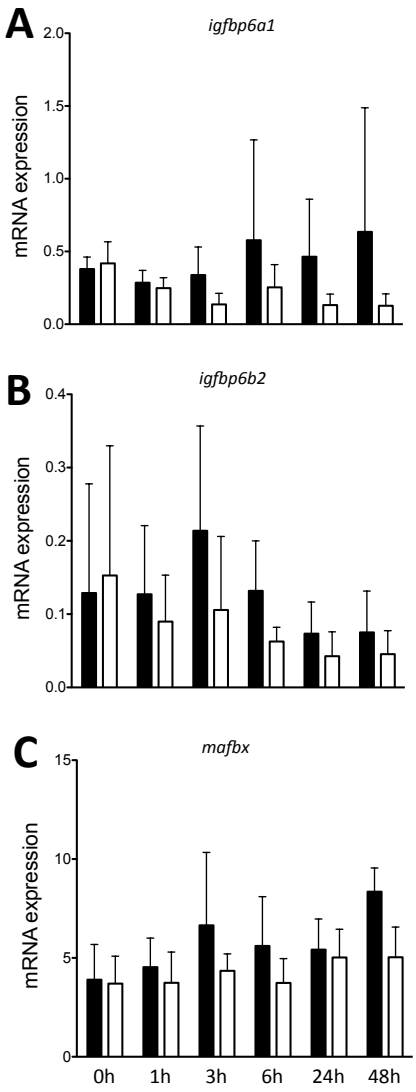

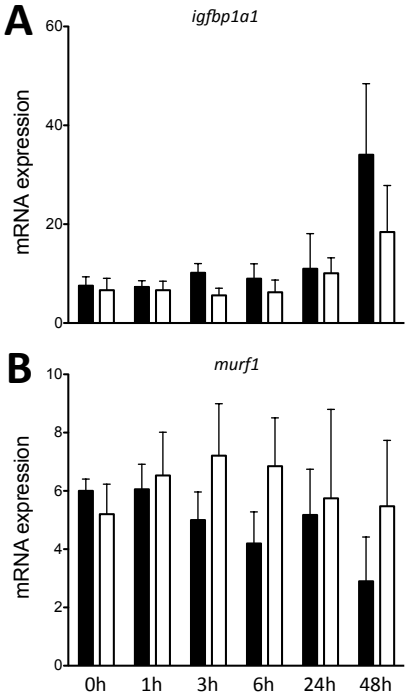

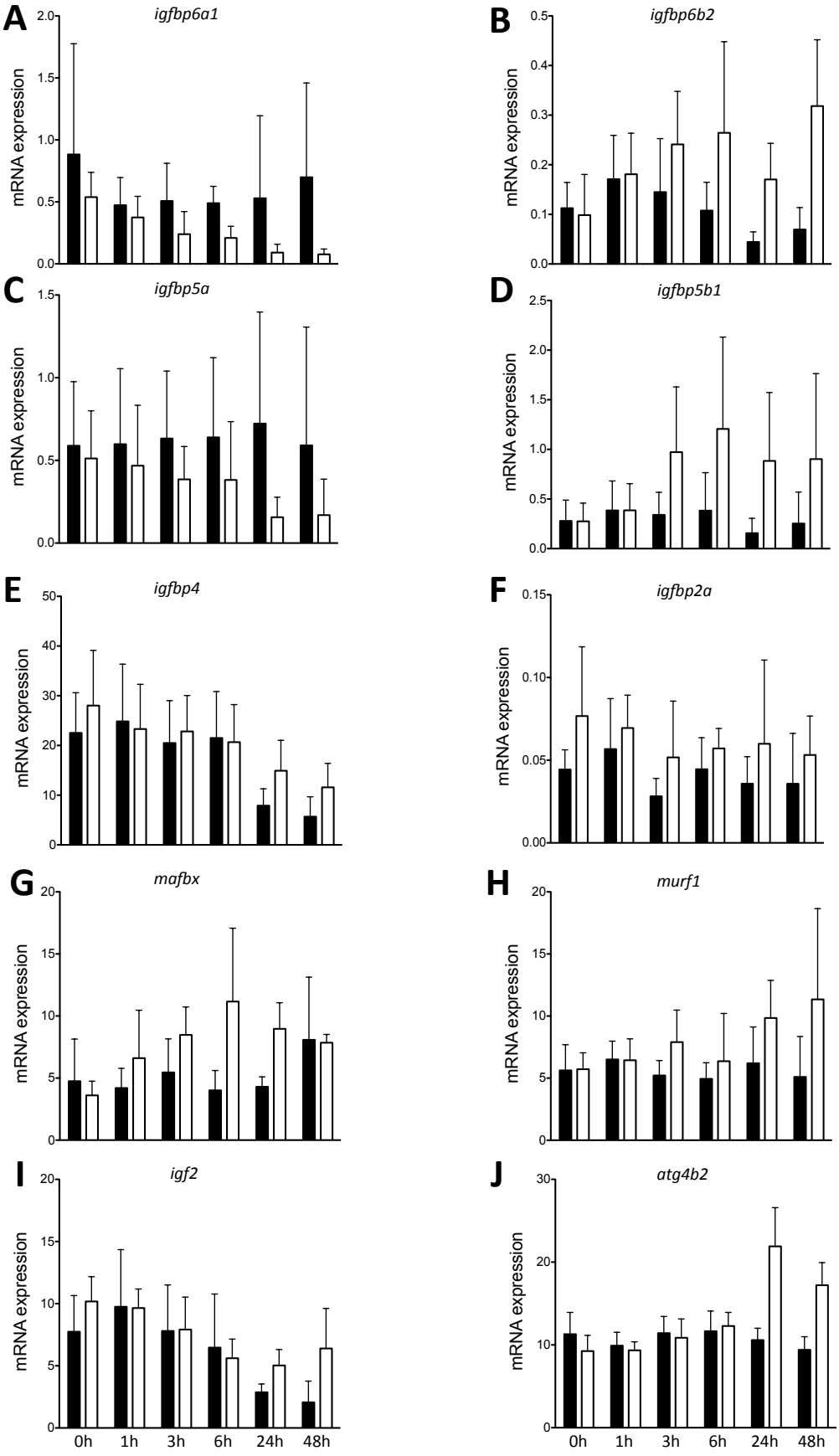

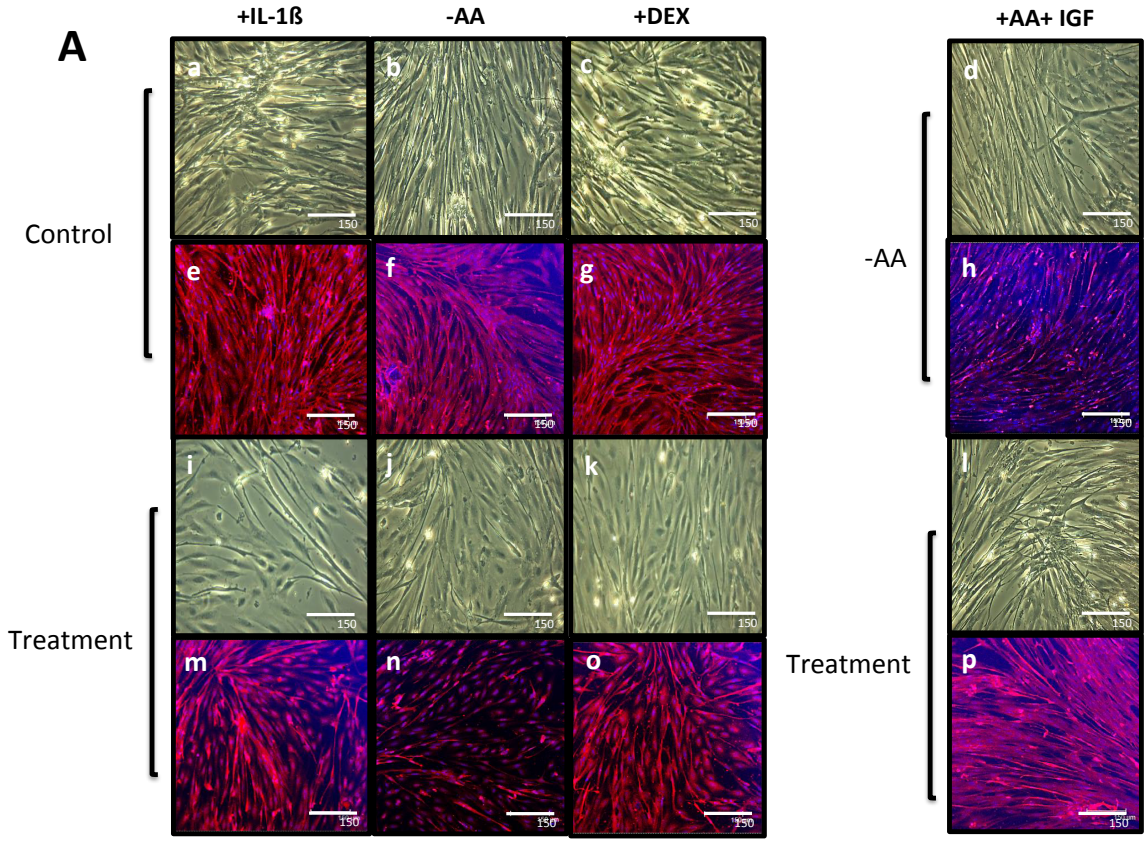

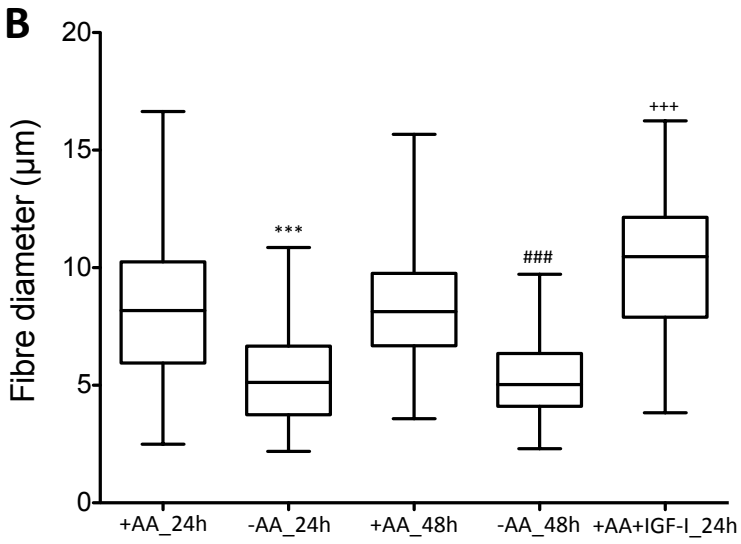

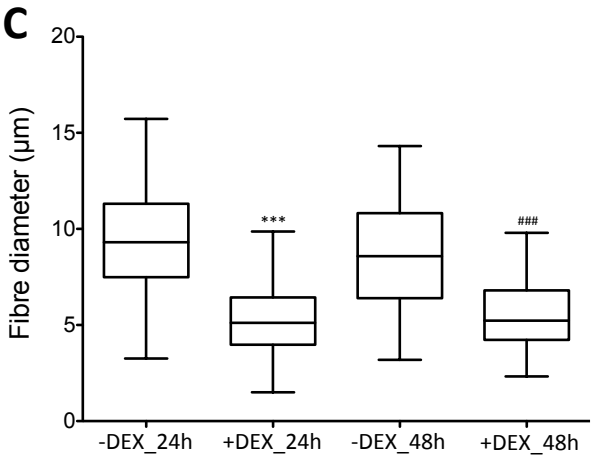

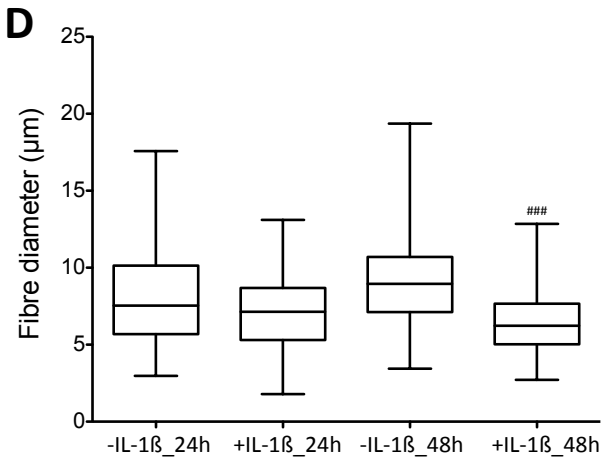

734

735

736

737 Table 1. Results of general linear modelling to investigate differences in gene expression in response to dexamethasone (+DEX) treatment
738

Gene	P-value Treatment	P-value Treatment *time-point	Transcript level 1 hour	+DEX / Control 1 hour	Transcript level 3 hour	+DEX / Control 3 hour	Transcript level 6 hour	+DEX / Control 6 hour	Transcript level 24 hour	+DEX / Control 24h	Transcript level 48 hour	+DEX / Control 48 hour
igfbp6a1	<0.0001	0.032	0.37(0.17)	0.79	0.24(0.18)	0.47	0.21(0.09)	0.43	0.09(0.07)	0.17	0.08(0.04)	0.11
igfbp6b2	<0.0001	0.005	0.18(0.08)	1.05	0.24(0.10)	1.66	0.26(0.18)	2.45	0.17(0.07)	3.83	0.31(0.13)	4.58
mafbx	<0.0001	0.054	6.60(3.86)	1.57	8.47(2.25)	1.55	11.16(5.9)	2.78	8.96(2.10)	2.08	7.84(0.66)	0.97
murf1	0.001	n/a	6.44(1.72)	0.99	7.90(2.58)	1.51	6.36(3.83)	1.28	9.84(3.02)	1.58	11.3(7.31)	2.22
igfbp5b1	0.002	n/a	0.38(0.26)	1.00	0.97(0.65)	2.85	1.20(0.92)	3.14	0.88(0.68)	5.65	0.90(0.86)	3.56
igf2	0.002	0.014	9.65(1.52)	0.99	7.91(2.60)	1.01	5.61(1.53)	0.86	5.03(1.28)	1.75	6.39(3.22)	3.09
igfbp2a	0.003	0.985	0.06(0.01)	1.22	0.05(0.03)	1.83	0.05(0.01)	1.28	0.05(0.05)	1.67	0.05(0.02)	1.48
atg4b2	0.003	<0.0001	9.35(1.02)	0.94	10.8(2.28)	0.95	12.28(1.64)	1.05	21.9(4.66)	2.06	17.2(2.73)	1.83
igfbp5a	0.007	0.443	0.46(0.36)	0.86	0.38(0.19)	0.60	0.38(0.35)	0.59	0.15(0.12)	0.21	0.16(0.21)	0.28
igfbp4	0.046	0.464	23.3(9.00)	0.93	22.8(7.22)	1.11	20.6(7.55)	0.96	14.9(6.13)	1.89	11.5(4.81)	2.03
atg4b1	0.100	0.082	13.0(2.96)	0.89	15.4(3.24)	0.91	21.4(5.20)	1.08	46.5(10.3)	1.56	43.0(7.94)	1.27
igfbp3a1	0.311	0.253	1.22(0.37)	0.89	0.95(0.32)	0.71	0.66(0.24)	0.51	0.98(0.53)	0.92	1.43(0.95)	1.24
igfbp1a1	0.464	0.814	14.2(4.29)	1.31	13.41(4.07)	1.19	12.9(5.56)	1.31	13.9(8.30)	0.85	28.8(16.8)	0.90
igfbp5b2	0.790	0.203	1.40(1.06)	1.05	2.37(1.90)	1.63	3.30(2.37)	1.80	1.03(0.50)	0.52	0.66(0.39)	0.17
myl1	0.859	n/a	12.9(13.9)	0.87	15.1(14.0)	1.12	10.7(9.40)	0.71	8.95(10.3)	0.73	9,71(11.1)	1.54
tnni1	0.969	0.864	0.22(0.18)	0.81	0.28(0.18)	1.03	0.23(0.10)	0.88	0.34(0.29)	1.07	0.48(0.39)	1.81

739
740 Genes showing a statistically significant response to dexamethasone (+DEX) treatment are underlined.
741 All values where the +DEX treatment is divided by the control show fold change in transcript levels
742 n/a: treatment*time-point interaction not assessed (Kruskal-Wallis test applied)
743
744
745

746

747

748 Table 2. Results of general linear modelling to investigate differences in gene expression in response to interleukin 1β (+IL-1β) treatment
749

Gene	P-value Treatment	P-value Treatment *time-point	Transcript level 1 hour	+IL-1β / Control 1 hour	Transcript level 3 hour	+IL-1β / Control 3 hour	Transcript level 6 hour	+IL-1β / Control 6 hour	Transcript level 24 hour	+IL-1β / Control 24h	Transcript level 48 hour	+IL-1β / Control 48 hour
igfbp1a1	0.003	0.556	6.64(1.83)	0.90	5.59(1.45)	0.54	6.24(2.45)	0.69	10.1(3.12)	0.91	18.4(9.41)	0.54
murf1	0.004	0.124	6.53(1.48)	1.07	7.21(1.78)	1.44	6.84(1.65)	1.63	5.74(3.05)	1.11	5.47(2.26)	1.88
igfbp3a1	0.128	0.796	0.87(0.34)	0.88	0.67(0.28)	0.51	0.49(0.06)	0.64	0.73(0.42)	1.09	0.55(0.29)	0.72
igfbp6a1	0.157	0.150	0.14(0.05)	0.83	0.24(0.18)	1.02	1.15(1.22)	2.22	0.79(0.43)	2.66	0.69(0.51)	1.39
igfbp5b2	0.181	0.955	0.90(0.63)	0.85	1.07(0.61)	0.47	1.50(0.83)	0.65	1.71(0.81)	1.05	1.47(0.87)	0.53
atg4b1	0.222	n/a	7.75(1.20)	0.89	8.73(0.93)	0.77	13.3(2.89)	0.86	22.3(7.94)	1.17	18.3(7.84)	0.87
igfbp5b1	0.284	0.675	0.27(0.14)	0.92	0.38(0.34)	1.02	0.46(0.48)	1.33	0.21(0.16)	1.39	0.17(0.14)	2.60
igfbp4	0.386	0.951	16.1(5.15)	0.92	13.9(4.09)	0.69	12.0(2.48)	0.95	7.41(4.5)	1.36	2.68(1.50)	0.73
igfbp2a	0.542	0.917	0.06(0.02)	0.88	0.05(0.02)	1.25	0.05(0.01)	0.99	0.05(0.02)	1.31	0.03(0.02)	0.97
igfbp6b2	0.581	0.695	0.10(0.07)	0.95	0.07(0.06)	0.41	0.07(0.05)	0.80	0.05(0.02)	0.76	0.05(0.02)	1.59
tnni1	0.646	n/a	0.27(0.18)	1.05	0.26(0.16)	0.91	0.33(0.26)	1.23	0.38(0.28)	1.07	0.28(0.17)	0.93
igf2	0.680	n/a	5.97(3.74)	1.20	4.48(2.05)	0.72	2.64(1.13)	1.06	1.81(1.13)	1.26	1.30(0.39)	1.01
atg4b2	0.700	0.213	9.69(1.41)	0.97	10.3(0.71)	0.83	14.3(2.61)	1.05	12.9(5.14)	0.93	12.6(4.28)	1.14
igfbp5a	0.756	0.977	0.17(0.11)	1.14	0.24(0.18)	0.96	0.21(0.18)	1.31	0.15(0.09)	1.15	0.12(0.07)	0.53
mafbx	0.791	0.507	3.54(1.04)	1.09	4.02(0.88)	0.62	5.24(2.68)	1.13	4.80(1.88)	1.02	5.22(1.76)	0.79
myl1	0.938	0.999	10.8(8.10)	1.03	10.8(8.45)	1.09	12.6(15.7)	1.60	8.59(8.30)	0.98	5.07(3.27)	1.17

750
751 Genes showing a statistically significant response to interleukin 1ß (+IL-1β) treatment are underlined.
752 All values where the +IL-1β treatment is divided by the control show fold change in transcript levels
753 n/a: treatment*time-point interaction not assessed (Kruskal-Wallis test applied)
754
755

Table 3. Results of general linear modelling to investigate differences in gene expression in response to amino acids deprivation (-AA) treatment

Gene	P-value Treatment	P-value Treatment *time-point	Transcript level 1 hour	-AA / Control 1 hour	Transcript level 3 hour	-AA / Control 3 hour	Transcript level 6 hour	-AA / Control 6 hour	Transcript level 24 hour	-AA / Control 24h	Transcript level 48 hour	-AA / Control 48 hour
igfbp6a1	<0.0001	0.136	0.24(0.07)	0.87	0.13(0.07)	0.40	0.25(0.15)	0.43	0.13(0.07)	0.28	0.12(0.08)	0.20
mafbx	0.012	0.679	3.74(1.55)	0.82	4.34(0.87)	0.65	3.73(1.22)	0.66	5.02(1.42)	0.92	5.03(1.52)	0.60
igfbp6b2	0.039	0.747	0.08(0.06)	0.70	0.10(0.10)	0.49	0.06(0.02)	0.47	0.04(0.03)	0.58	0.04(0.03)	0.60
igfbp5a	0.056	n/a	0.26(0.19)	1.00	0.22(0.19)	0.68	0.28(0.28)	0.74	0.20(0.24)	0.60	0.06(0.08)	0.17
murf1	0.083	0.734	8.90(3.10)	1.19	9.85(1.64)	1.32	10.3(5.44)	1.26	8,14(3.20)	0.96	11.7(7.73)	2.07
atg4b2	0.092	0.569	8.06(1.58)	1.08	7.92(1.78)	0.97	7.14(3.26)	0.71	8,21(2.72)	0.74	5.95(1.74)	0.72
igfbp3a1	0.098	0.154	1.90(1.30)	0.88	1.68(0.52)	0.75	1.89(0.40)	1.14	3.61(1.84)	1.89	5.10(2.75)	2.35
atg4b1	0.107	0.744	9,56(3.54)	1.09	10.1(2.75)	0.94	10.6(3.18)	0.73	16,3(5.67)	0.68	15.2(6.40)	0.68
myl1	0.307	0.653	19.1(17.6)	1.38	16.4(16.0)	1.23	12.5(13.4)	0.78	7.00(8.06)	0.45	2.62(1.78)	0.43
tnni1	0.314	0.911	0.50(0.40)	1.19	0.40(0.25)	0.99	0.35(0.24)	0.72	0.38(0.37)	0.71	0.25(0.15)	0.73
igfbp2a	0.392	0.919	0.10(0.03)	0.97	0.07(0.02)	0.88	0.07(0.02)	1.12	0.05(0.02)	0.94	0.04(0.01)	0.72
igf2	0.409	0.504	5.94(5.64)	0.73	4.64(3.30)	0.63	6.33(4.68)	1.58	3.37(2.04)	1.25	5.39(5.36)	2.22
igfbp1a1	0.627	0.304	18.6(9,98)	0.94	17.84(7.92)	0.98	17.6(5.14)	1.11	25.4(9.43)	1.18	35.9(12.8)	0.63
igfbp4	0.649	n/a	30.2(20.7)	0.80	29,9(20.3)	0.84	31.8(18.9)	1.20	16.8(9.91)	1.38	12.5(5.74)	1.88
igfbp5b1	0.843	0.814	0.08(0.04)	0.94	0.100(0.08)	0.98	0.08(0.08)	0.56	0.06(0.05)	1.13	0.03(0.02)	1.06
igfbp5b2	0.901	0.994	0.50(0.57)	0.88	0.61(0.59)	0.74	1.38(1.14)	1.27	1.09(0.98)	1.24	1.15(1.06)	0.54

Genes showing a statistically significant response to amino acids deprivation (-AA) treatment are underlined.
All values where the -AA treatment is divided by the control show fold change in transcript levels
n/a: treatment*time-point interaction not assessed (Kruskal-Wallis test applied)

Table 4. Results of general linear modelling to investigate differences in gene expression in response to adding amino acids and Igf-I growth factor (+AA +Igf-I) treatment.

Gene	P-value Treatment	P-value Treatment *time-point	Transcript level 48 hour*	+AA +Igf-I / Control 48 hour*	Transcript level 1 hour	-AA / Control 1 hour	Transcript level 3 hour	-AA / Control 3 hour	Transcript level 24 hour	-AA / Control 24h
mafbx	<0.0001	0.073	5.03(1.52)	0.60	0.87(0.35)	0.31	0.59(0.26)	0.28	0.98(0.45)	0.55
atg4b2	0.001	0.186	5.95(1.74)	0.71	31.96(8.12)	0.78	25.03(6.15)	0.57	27.80(11.3)	0.78
igfbp4	0.002	0.888	12.5(5.74)	1.88	11.36(5.46)	2.09	14.1(7.5)	2.72	7.76(6.04)	2.82
igf2	0.009	0.824	5.39(5.36)	2.21	10.9(2.68)	1.76	10.9(5.64)	1.85	2.86(1.78)	1.49
igfbp6b2	0.010	0.171	0.05(0.01)	0.75	1.04(1.23)	3.80	0.29(0.14)	1.35	0.12(0.07)	1.56
igfbp5b1	0.016	0.354	0.03(0.02)	1.06	0.64(0.66)	2.67	0.66(0.87)	2.12	0.27(0.19)	1.54
igfbp1a1	0.021	0.760	35.0(12.8)	0.63	7.63(5.65)	0.43	10.1(6.46)	0.68	10.1(5.3)	0.77
atg4b1	0.033	n/a	15.2(6.24)	0.68	5.03(0.90)	0.59	3.78(0.92)	0.45	6.85(4.51)	0.90
igfbp5a	0.086	n/a	0.08(0.07)	0.21	0.16(0.05)	1.46	0.26(0.09)	1.65	0.12(0.07)	4.84
igfbp2a	0.514	0.626	0.04(0.01)	0.72	0.02(0.004)	1.48	0.02(0.01)	1.47	0.02(0.009)	1.43
murf1	0.608	0.057	11.78(7.73)	2.07	3.59(1.28)	0.81	2.16(1.33)	0.61	3.33(1.33)	0.69
tnni1	0.689	0.534	0.25(0.15)	0.73	0.27(0.18)	0.77	0.27(0.19)	0.76	0.99(0.71)	1.84
igfbp5b2	0.834	0.404	1.15(1.06)	0.54	0.20(0.21)	0.96	0.15(0.10)	0.71	0.58(0.48)	1.88
igfbp3a1	0.875	0.063	5.10(2.75)	2.35	1.03(0.68)	1.44	0.65(0.34)	0.85	0.47(0.25)	0.74
igfbp6a1	0.877	0.029	0.12(0.08)	0.20	0.12(0.04)	0.84	0.32(0.27)	2.30	0.66(1.09)	4.24
myl	0.879	n/a	2.62(1.78)	0.43	8.98(12.75)	0.95	12.8(18.4)	1.19	13.5(15.2)	0.98

* refers to myotubes being maintained for 48 hours in media free of amino acids for 48 hour before adding amino acids and Igf-I growth factor (+AA +Igf-I) treatment
Genes showing a statistically significant response to +AA +Igf-I treatment are underlined.
All values where the +AA +Igf-I treatment is divided by the control show fold change in transcript levels
n/a: treatment*time-point interaction not assessed (Kruskal-Wallis test applied).